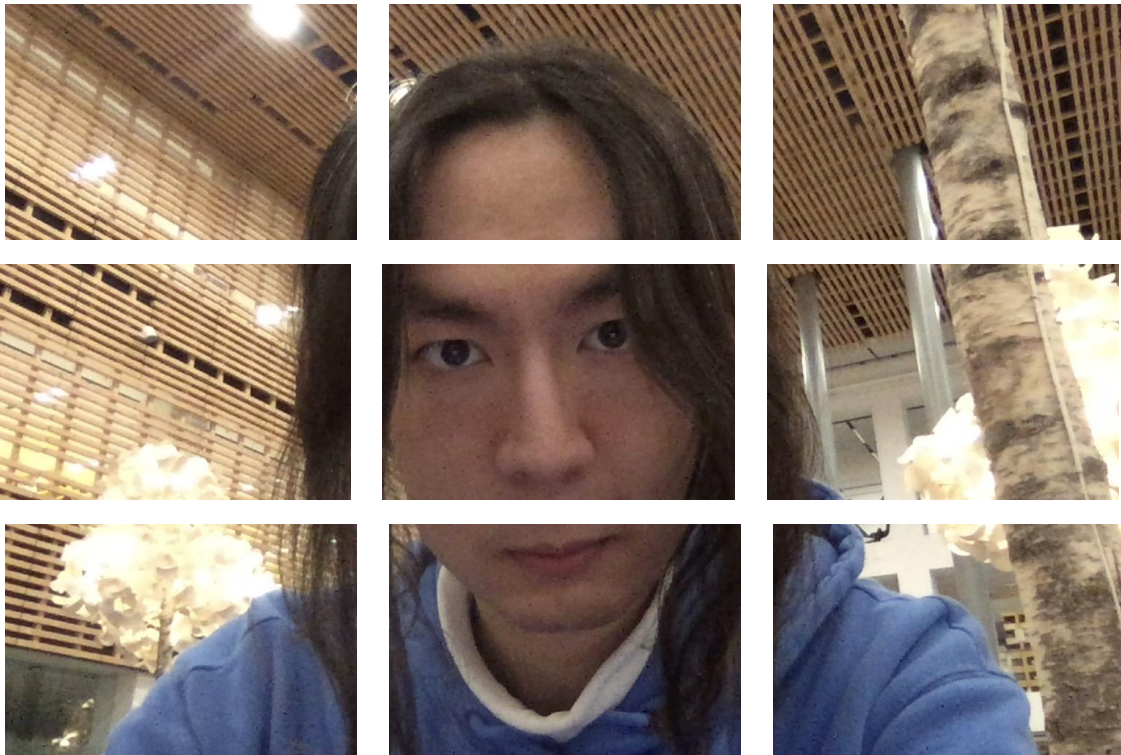# Problem Set #3

## Advanced Methods in Applied Statistics

**Cyan Yong Ho Jo**
13th March 2024

## EX1

### Quick look

The training dataset comprises four features: age, education, gender, and working hours per week. Initially, I opt to examine the data distribution concerning these features, which are depicted in Figures 1, 2, 3, and 4, respectively. Subsequently, I establish a null hypothesis for the classification, positing that the classified groups earn more than 50k. Consequently, the alternative hypothesis posits that the other group earns 50k or less. A quick investigation of the data impresses me that discerning the dataset into two distinct groups might not be simple or intuitive. So I shall consider utilising several classifiers instead of one. My selected classifiers include the following four: Adaptive Boosting, Logistic Regression, XGB, and Gradient Boosting.
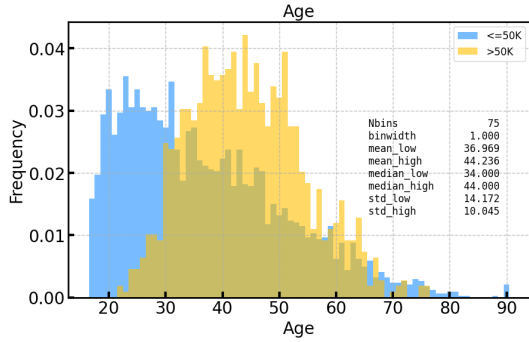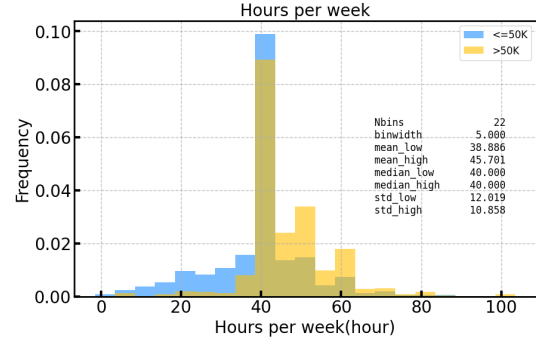


**Figure 1:** The distribution of groups earning less than 50k and more than 50k, categorized by age. Each histogram bar is binned in intervals of 1
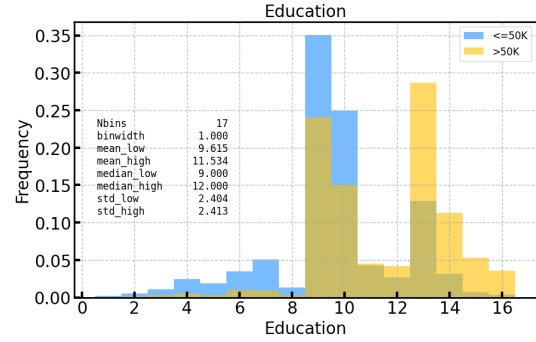


**Figure 2:** The distribution of groups earning less than 50k and more than 50k, categorized by education. Each histogram bar is binned in intervals of 1.
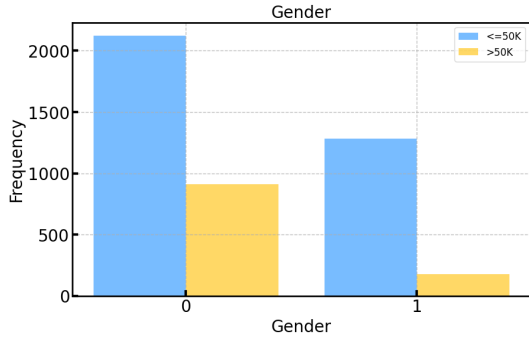


**Figure 3:** The distribution of groups earning less than 50k and more than 50k, categorized by gender.



**Figure 4:** The distribution of groups earning less than 50k and more than 50k, categorized by the working hours per week. Each histogram bar is binned in intervals of 5 hours.

### Classification

To train a classifier, the dataset must be divided into two subsets, each serving a distinct purpose: a training set and a test set. This division is executed by the train_test_split function from the sklearn.model_selection module in Python, which utilises a random selection process to segregate the data. Both high-earners and low-earners must be represented by more than 500 data points each. Given the smaller number of high-earning individuals, particular attention is paid to the size of the high-earning group. The proportion of the test group is set to 45% of the total dataset. Consequently, within the testing group of 2025 individuals, there are 506 high-earners.

*Overtraining check*

Since there is no guarantee that the dataset is not overtrained, comparing the training and testing sets is crucial. The outcome of this comparison is illustrated in TableI. The classifier now scores each data item against a given threshold. Setting thresholds for classifiers is challenging due to the different distributions of decision scores produced by each classifier. A function is defined to find the optimal threshold, however, it is required to adjust the threshold manually based on visual inspection of histograms. The precision achieved by each classifier is then determined. Algorithms such as Adaptive Boosting, XGB, and Gradient Boosting meet the precision criteria. Logistic Regression, however, fails to meet the 85% condition. These precisions are summarised in TableII.

| | > 50k | | ≤ 50k | |
| | Test Group | Train Group | Test Group | Train Group |
|---|---|---|---|---|
| **Mean** | 43.70 | 44.70 | 36.67 | 37.21 |
| **Median** | 44 | 43 | 34 | 35 |
| **Std Dev** | 9.92 | 10.14 | 14.35 | 14.02 |
| **Mean** | 11.49 | 11.57 | 9.63 | 9.60 |
| **Median** | 12 | 12 | 9 | 9 |
| **Std Dev** | 2.39 | 2.43 | 2.43 | 2.38 |
| **Mean** | 45.77 | 45.64 | 38.98 | 38.81 |
| **Median** | 40 | 44 | 40 | 40 |
| **Std Dev** | 10.51 | 11.16 | 11.99 | 12.05 |

Table I: **No sign of overtraining.** Basic statistics of the test and train groups will be classified into two groups by four different classifiers. The training and testing groups have similar statistical characteristics. Comparing the statistical character helps prevent overtraining.

| | **Adaptive boost** | **Logistic regression** | **XGB** | **Gradient boost** |
|---|---|---|---|---|
| Precision | 85.71% | 81.48% | 88.89% | 89.29% |

Table II: Precision of the classifications by the four different classifiers.

*Confusion matrix and decision scores*

The confusion matrix results from classification tasks, comprising counts of true negatives, false positives, false negatives, and true positives. These quantities evaluate the classifier's performance, and certain combinations of these values are employed to assess metrics such as precision. The confusion matrices for all classifications are tabulated in Table**??** and visualised in Figures5, 6, 7, and 8 respectively. For Adaptive boosting, working hours, age, and education show moderate differences in predicting the high-earners and low-earners, while gender is considered a bad variable to guess. For Logistic regression, however, gender marked the highest score for the differentiator. XGB says education is the most important feature while the second and the third most important features are gender and age having similar importance scores. Lastly, Gradient boost shows that the two most effective features are education and age in prediction. This is summarised in TableIV.

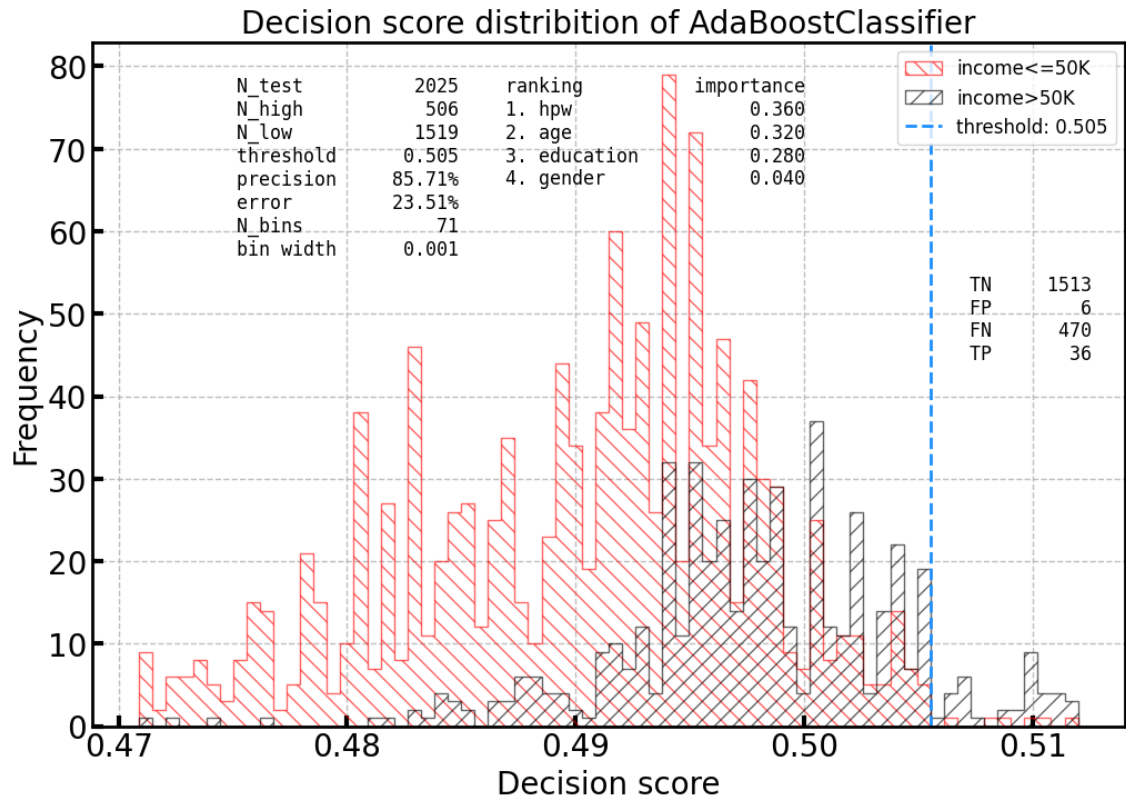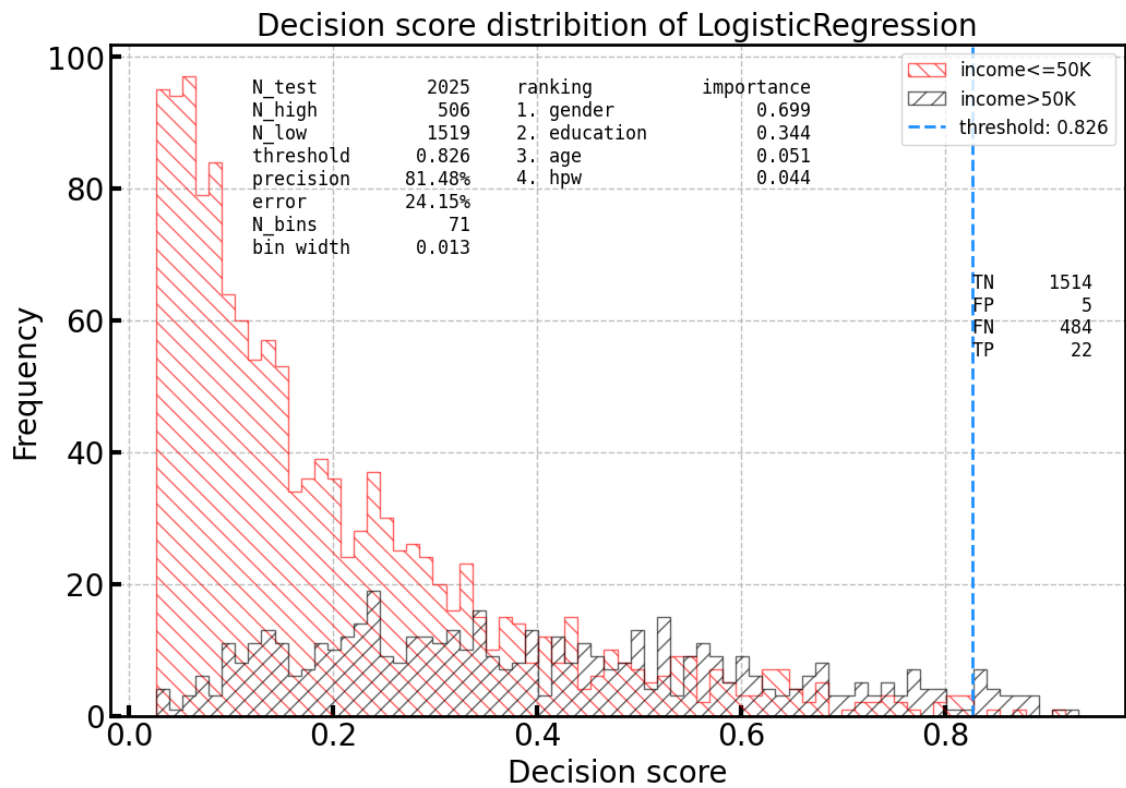| | Negative | Positive | | Negative | Positive | | Negative | Positive | | Negative | Positive |
|---|---|---|---|---|---|---|---|---|---|---|---|
| False | 470 | 6 | False | 484 | 5 | False | 482 | 3 | False | 481 | 3 |
| True | 1513 | 36 | True | 1514 | 22 | True | 1516 | 24 | True | 1516 | 25 |
| | Adaptive Boosting | | | Logistic regression | | | XGB classifier | | | Gradient Boosting | |

Table III: Confusion matrices for the classifications using Adaptive Boosting, Logistic Regression, XGBoost, and Gradient Boosting.
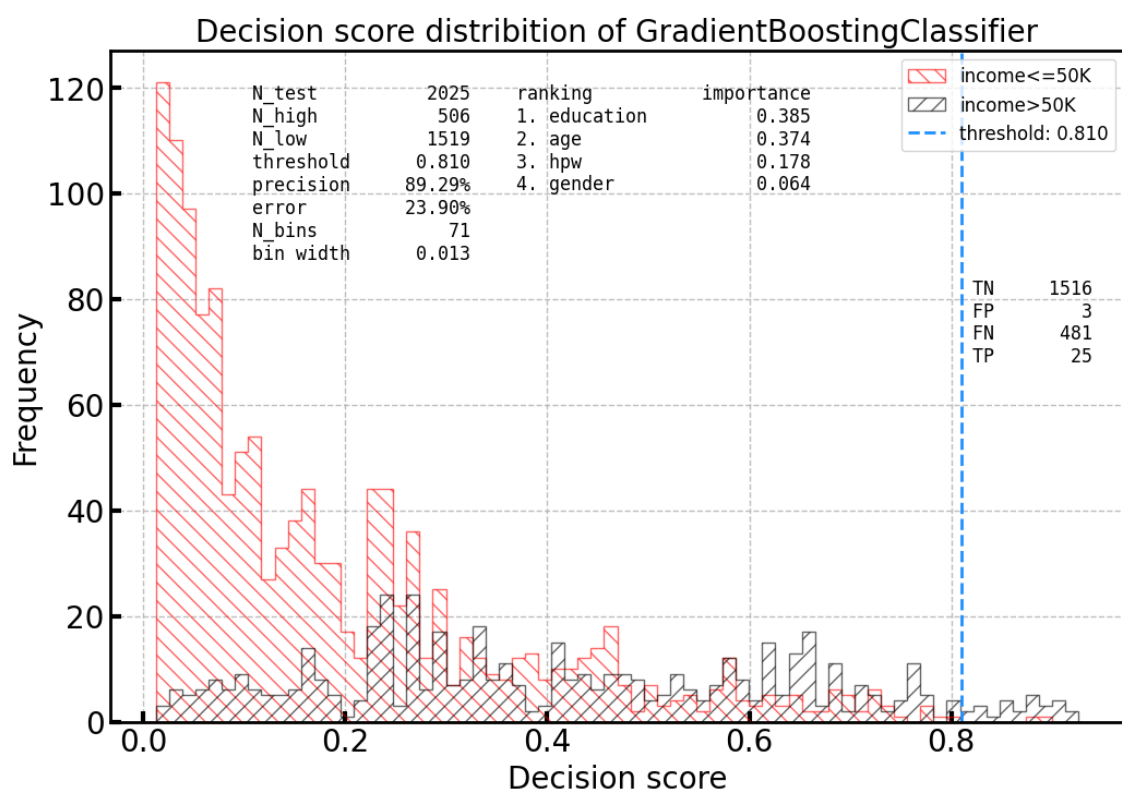
Decision score distribition of AdaBoostClassifier

| N_test | 2025 | ranking | importance |
| N_high | 506 | 1. hpw | 0.360 |
| N_low | 1519 | 2. age | 0.320 |
| threshold | 0.505 | 3. education | 0.280 |
| precision | 85.71% | 4. gender | 0.040 |
| error | 23.51% | | |
| N_bins | 71 | | |
| bin width | 0.001 | | |

| TN | 1513 |
| FP | 6 |
| FN | 470 |
| TP | 36 |

income<=50K
income>50K
threshold: 0.505

**Figure 5:** The Decision score distribution of the classification by Adaptive boost.

Decision score distribition of LogisticRegression

| N_test | 2025 | ranking | importance |
| N_high | 506 | 1. gender | 0.699 |
| N_low | 1519 | 2. education | 0.344 |
| threshold | 0.826 | 3. age | 0.051 |
| precision | 81.48% | 4. hpw | 0.044 |
| error | 24.15% | | |
| N_bins | 71 | | |
| bin width | 0.013 | | |

| TN | 1514 |
| FP | 5 |
| FN | 484 |
| TP | 22 |

income<=50K
income>50K
threshold: 0.826

**Figure 6:** The Decision score distribution of the classification by Logistic regression.

## Decision score distribution of XGBClassifier
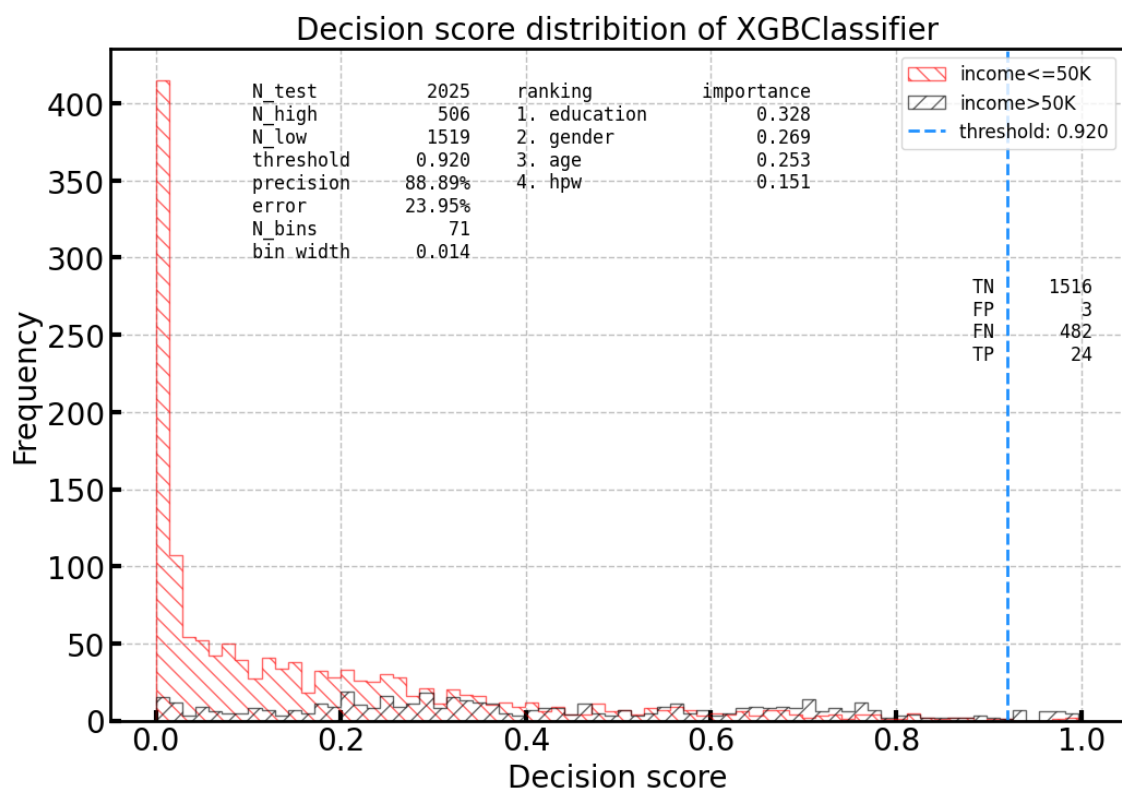


**Figure 7:** The Decision score distribution of the classification by XGB.

## Decision score distribition of GradientBoostingClassifier



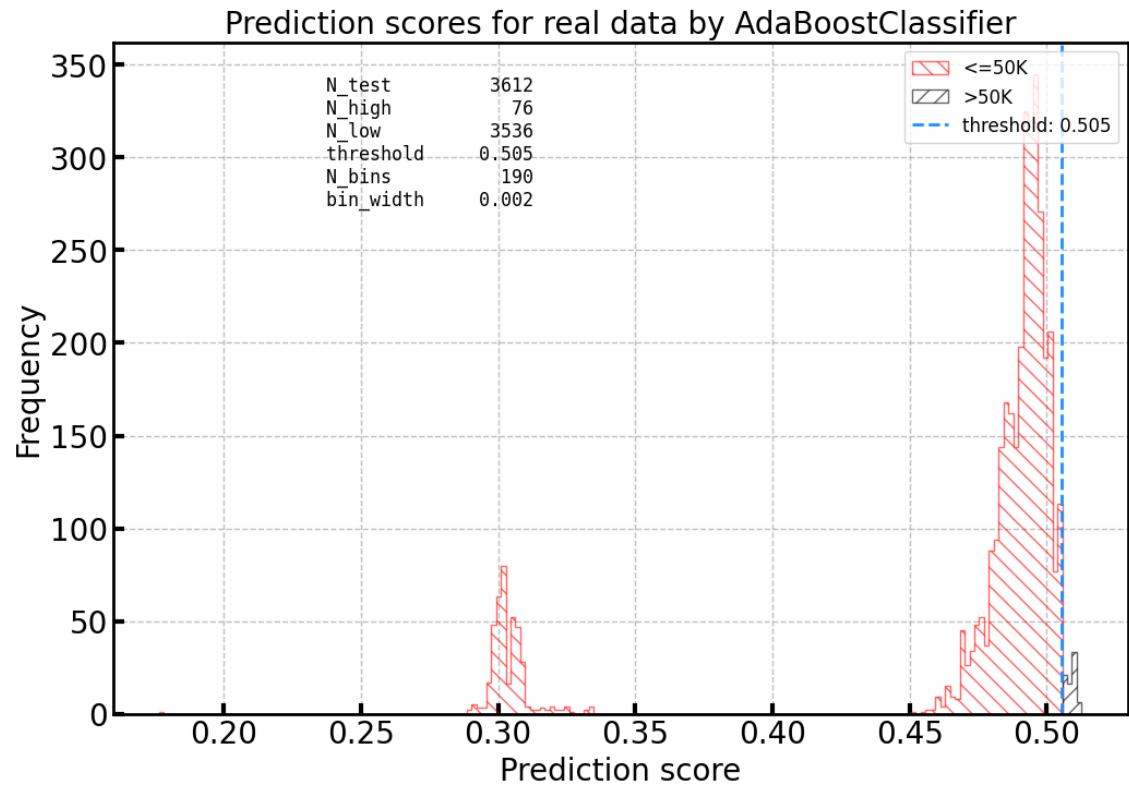**Figure 8:** The Decision score distribution of the classification by Gradient boost.

| | AdaBoost | Logistic Regression | XGBoost | Gradient Boosting |
|---|---|---|---|---|
| 1 | hpw: 0.360 | gender: 0.699 | education: 0.328 | education: 0.385 |
| 2 | age: 0.320 | education: 0.344 | gender: 0.269 | age: 0.374 |
| 3 | education: 0.280 | age: 0.051 | age: 0.253 | hpw: 0.178 |
| 4 | gender: 0.040 | hpw: 0.044 | hpw: 0.151 | gender: 0.064 |

**Table IV:** Feature importance ranking and scores for different classifiers

*Prediction on real data*

The real dataset is processed using four classifiers having the same thresholds that they used in training and testing. The resulting prediction scores are presented in Figure9, 10, 11, and 12.
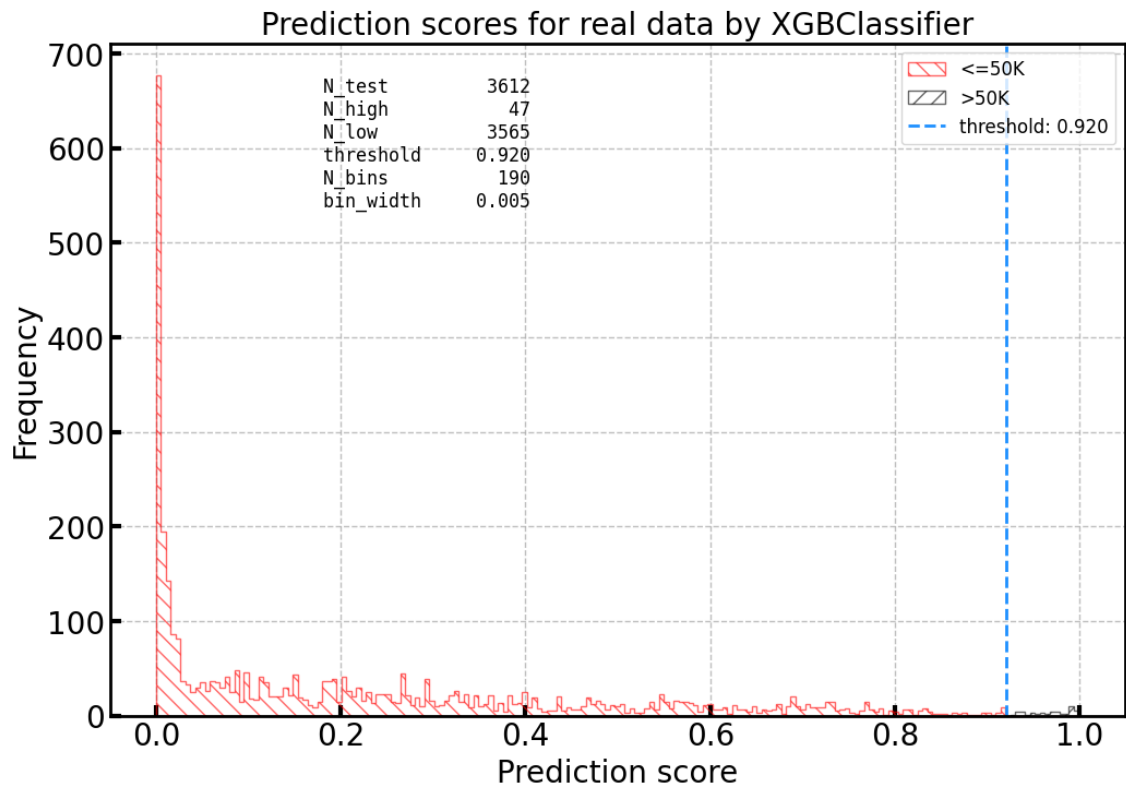


**Figure 9:** Distribution of prediction scores by Adaptive boost on real data, with the threshold indicating the decision boundary for income classification.
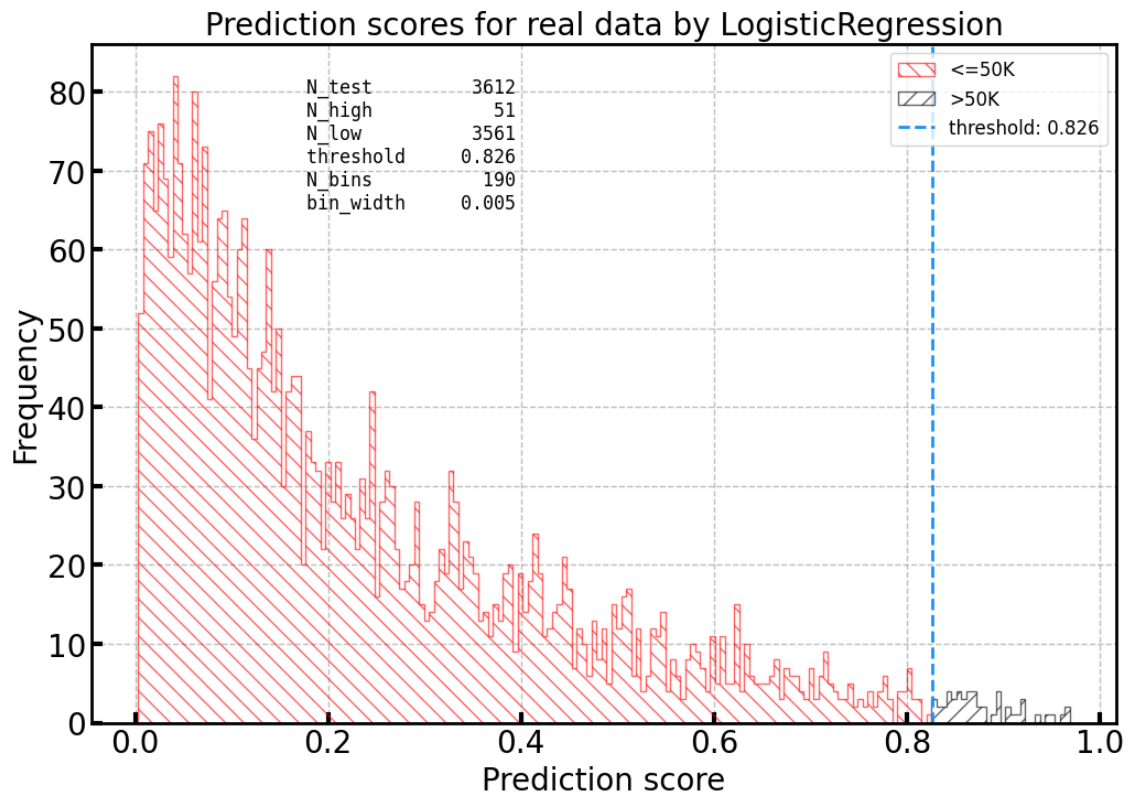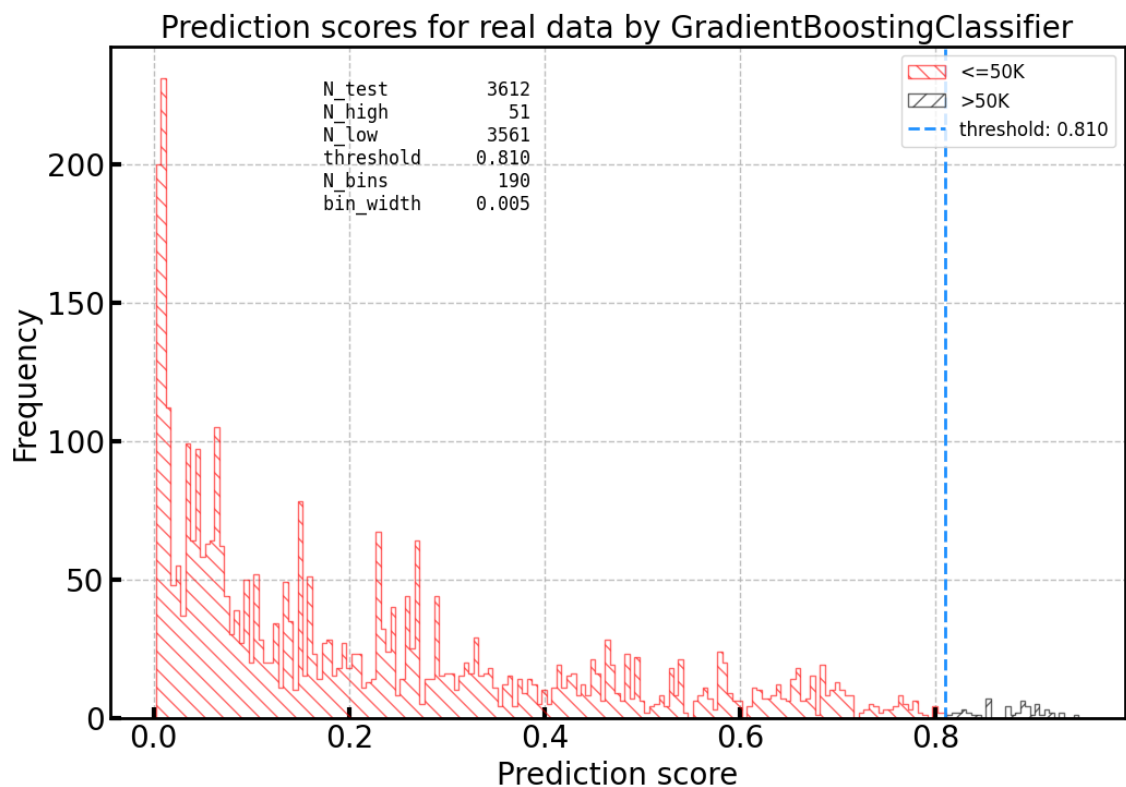
**Figure 10:** Logistic Regression's prediction score distribution on real data, with a marked threshold for classify ng incomes.

**Figure 11:** Prediction score distribution for real data using XGB, displaying the threshold for income predictions.



**Figure 12:** Gradient Boosting's prediction scores for real data, with the threshold delineating the classification of income levels.

Total: 4/4
Excellent

**EX2**

**Scatter of car accidents**

The *lat*, *lon*, and *crash_date* columns of data contain some missing values, so the rows missing the longitude, latitude, and time should be removed before data processing. *crash_date* column has string format of date and time so the data in that column need to be parsed in numerical format.
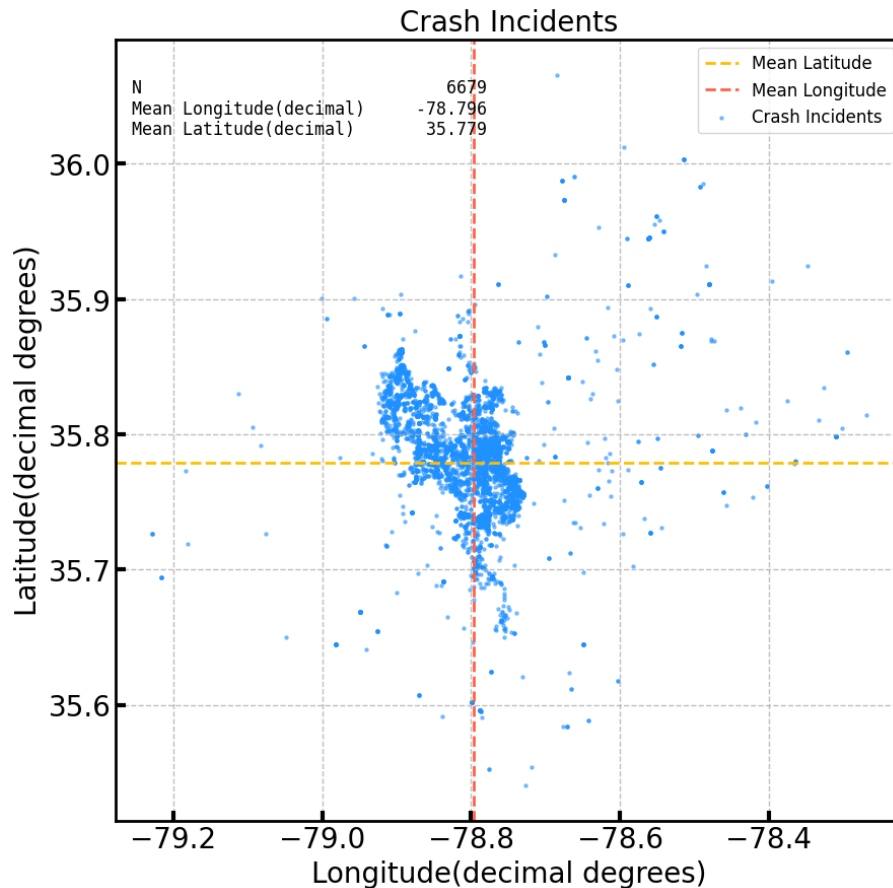


**Figure 13:** The scatter plot of the car accidents in the given data.

**Histogram of time and Gaussian KDE**

Since the daily time cycle repeats every 24 hours, the histogram's x-axis can be viewed as a loop. Thus, the data from either end of the axis, near 00:00 and 23:59, could be connected to the other side. Here the initially parsed data is plotted in Figure14. Manipulating the histogram to be adjusted such that its peak is centred horizontally. The adjusted histogram in Figure15 exhibits a dominant bell-shaped distribution with some hints of several minor peaks that may contribute to the total profile. By applying the Gaussian formula to each time data point in the adjusted histogram, we generate a Gaussian KDE that reflects the underlying distribution of the time-based events.
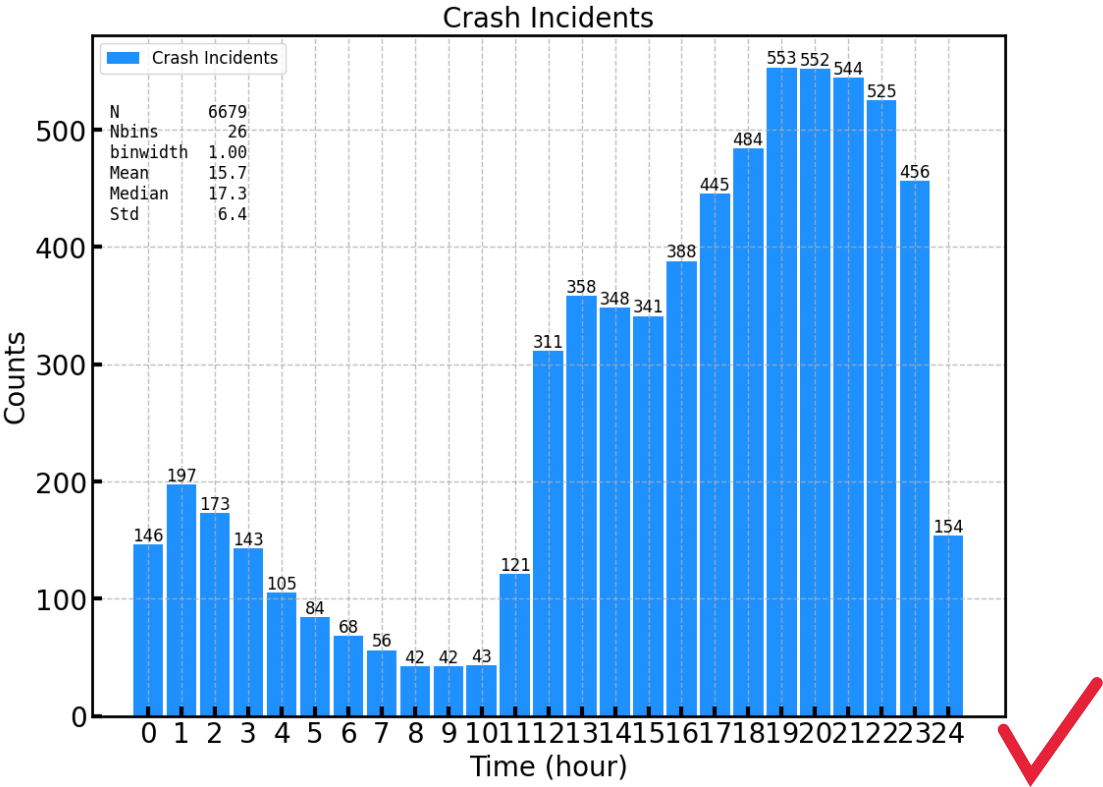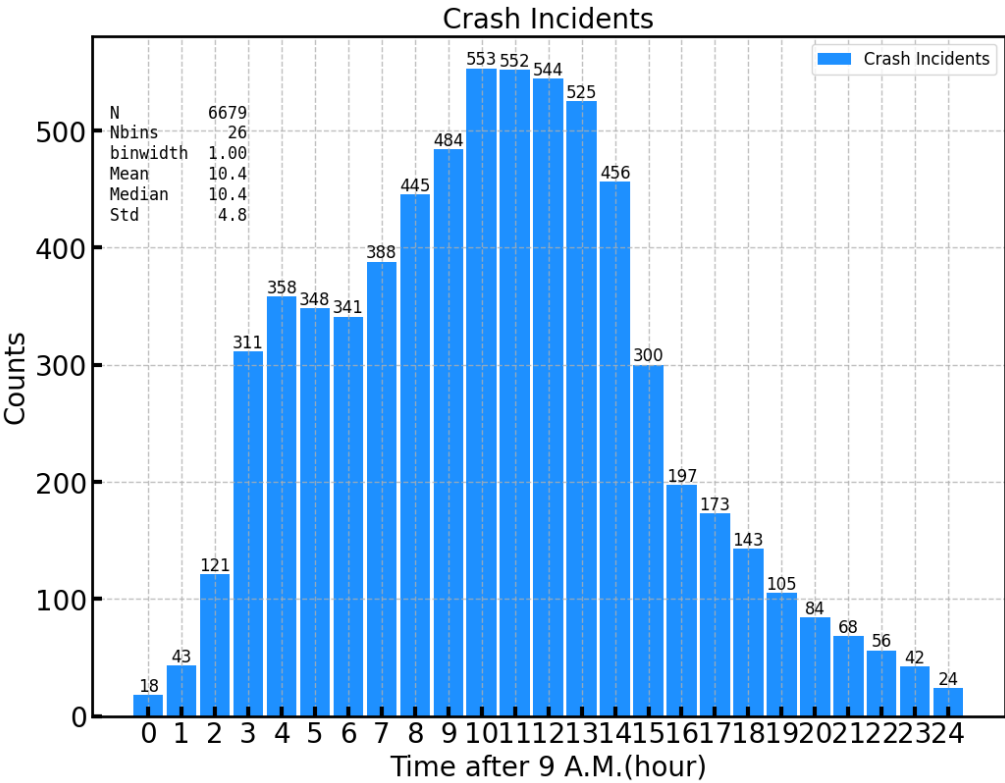
**Figure 14:** First figure



**Figure 15:** Second figure
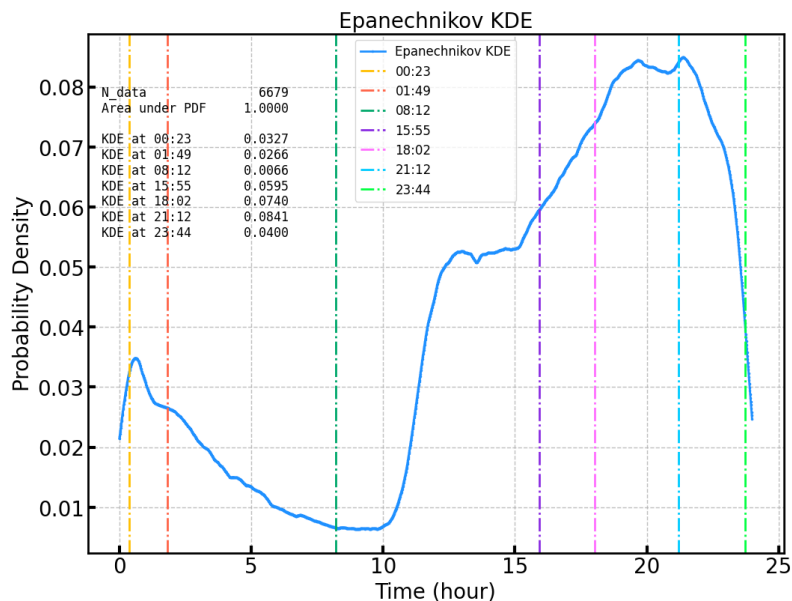
### Epanechnikov KDE for time

An Epanechnikov kernel density function is manually defined to calculate the values at each point. Summing up the values calculated by that function at each point and dividing by the total area will give a PDF or KDE. There are two data layouts that I used to give as the input to the function. One is the original distribution of the car accident and the other is the modification in the way I build Figure 15. As they have different distributions, KDE values are also slightly different. Figure16 shows the Epanechnikov KDE in its original distribution. Figure 17 shows the KDE of the modified data distribution. TableV as well as in the two figures.

### Optimal patrol starting point

To optimise the start time for a two-hour patrol, I aggregated the KDE values within two-hour intervals. This is visualized in Figures 16 and 17, showing the sum of KDE values for each potential start time throughout the day. The analysis aimed to identify the period with the highest likelihood of activity, as indicated by the KDE values. The optimal patrol start time is 19:33 which is marked by a dashed vertical line in Figure 17, suggesting the most advantageous time to commence the patrol based on the data.

| Time | KDE original | KDE modified |
|------|--------------|--------------|
| 00:23 | 0.0327 | 0.0392 |
| 01:49 | 0.0266 | 0.0263 |
| 08:12 | 0.0660 | 0.0065 |
| 15:55 | 0.0595 | 0.0588 |
| 18:02 | 0.0740 | 0.0732 |
| 21:12 | 0.0841 | 0.0832 |
| 23:44 | 0.0400 | 0.0511 |

**Table V:** KDE Values at Specified Time Points



**Figure 16:** The original Epanechnikov KDE values over 24 hours. Each vertical line corresponds to a specific time point, and the height of the curve represents the KDE value, indicating the probability density of events.
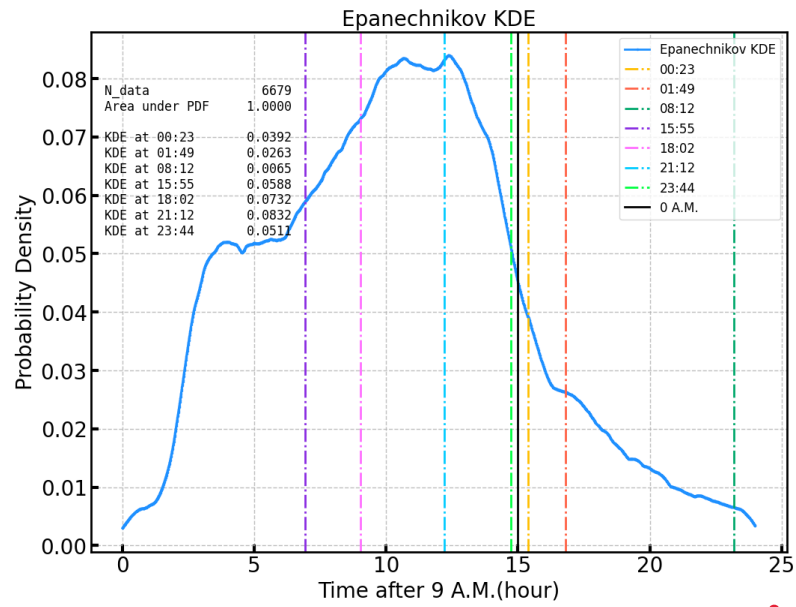
**Figure 17:** The modified Epanechnikov KDE values over 24 hours. Each vertical line corresponds to a specific time point, and the height of the curve represents the KDE value, indicating the probability density of events.
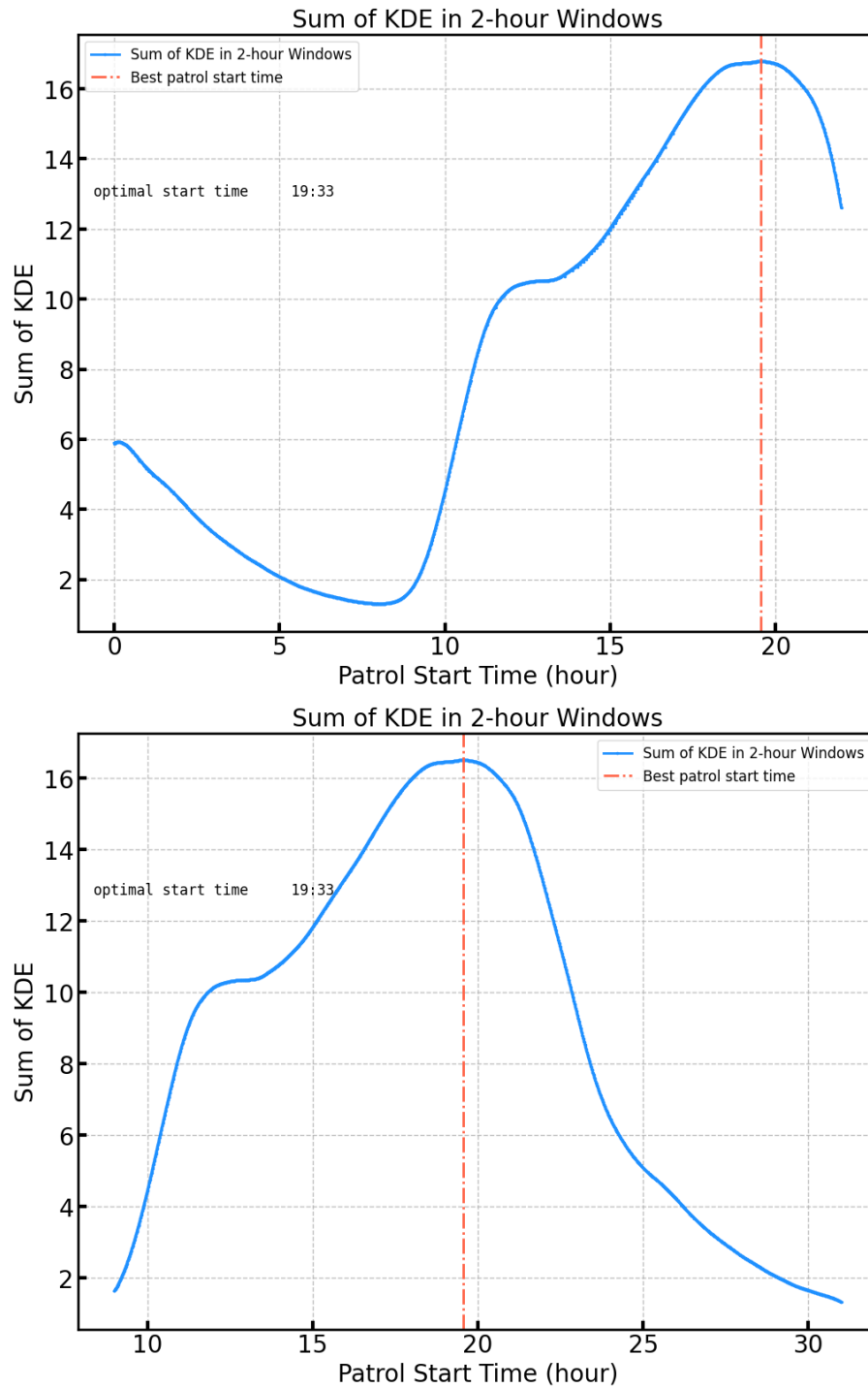
**Figure 18:** Cumulative sum of KDE values in two-hour windows plotted against potential patrol start times. The dashed vertical line indicates the optimal start time for a patrol, determined by the peak of the aggregated KDE values. The top panel is for the original KDE and the bottom is for the modified KDE.
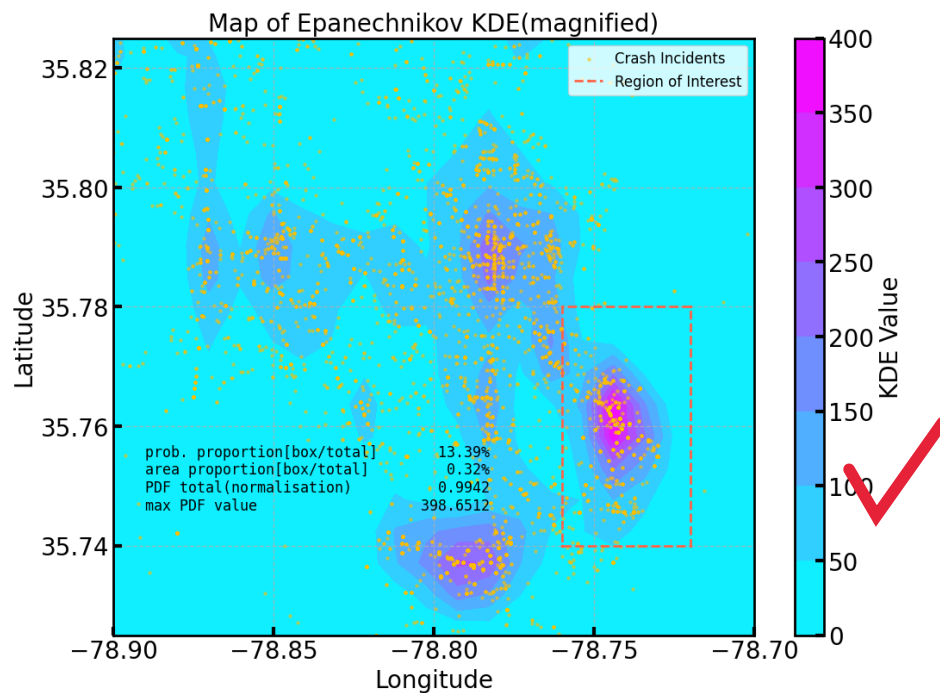
**Epanechnikov KDE map**

The geographic distribution of Epanechnikov Kernel Density Estimate (KDE) values is depicted in Figure 19, which illustrates a broad view across various latitudes and longitudes. A region of interest is demarcated with a dashed line, where the concentration of KDE values is noticeably

higher. In Figure 20, this region of interest is magnified to provide a closer examination of the spatial distribution of the KDE values. The proportion of the probability within the boxed region is significant at 13.39%, particularly when considering that this region covers only a small fraction of the map's total area a mere 0.32%. This high probability density in a relatively minuscule area indicates a substantial clustering of the data points of interest, likely corresponding to a higher frequency or intensity of the studied phenomenon in that specific location.
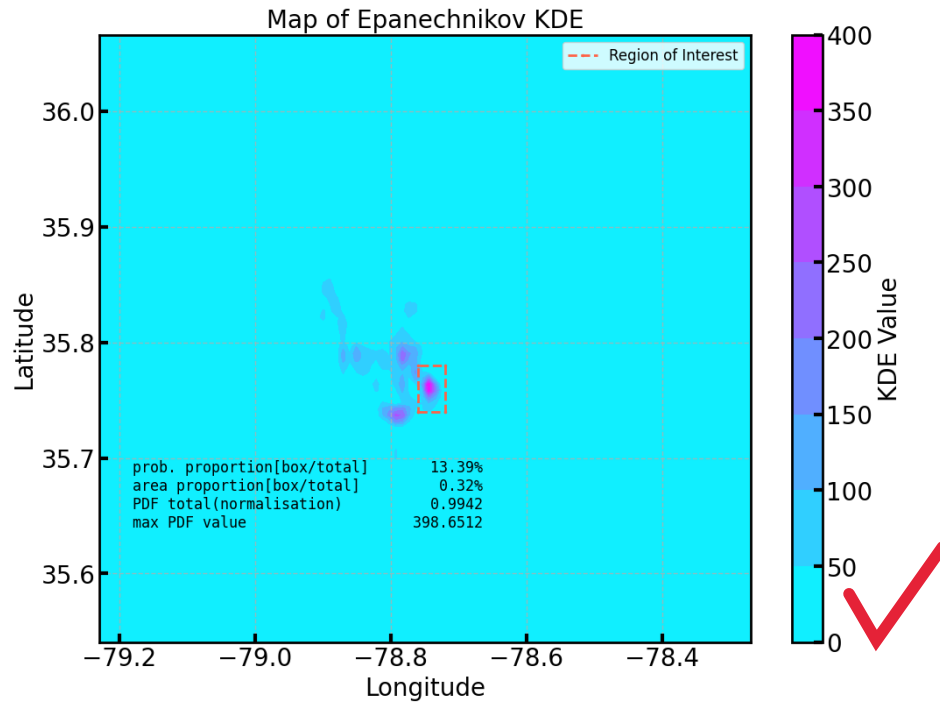
**Figure 19:** The geographical map representing the Epanechnikov KDE values. A dashed line encloses the region of interest, highlighting an area with a relatively high density of the accidents across the latitude and longitude coordinates.



**Figure 20:** A magnified view of the region of interest within the geographical map of Epanechnikov KDE values. The coloured points represent the accidents, emphasising the concentration of events within this locale.
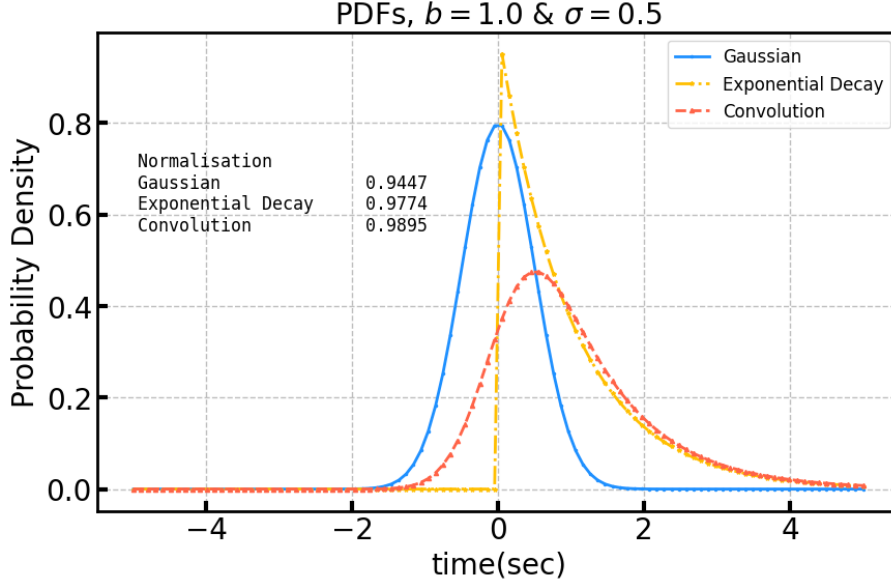
Total: 4/4
Wonderful

**EX3**

**The convolution of the PDFs**

The calculation of the convolution of two PDFs is computationally demanding since it entails definite integration. The Gaussian, and exponential decay and their convolution are plotted in Figure21. They all are PDFs so they must be normalised.



**Figure 21:** The figure displays three probability density functions (PDFs): the exponential decay and Gaussian distributions, considered seed PDFs with initial guess values of $b = 1$ and $\sigma = 0.5$. The red curve represents the convolution of these two seed PDFs, resulting in another PDF. The normalisation of all three PDFs has been verified.

**Calculating likelihood and finding minimum**

For hypothesis testing, I consider a null hypothesis where $b = 1$ and an alternative hypothesis where $b \neq 1$. To determine the most probable values of the remaining free parameters $b$(for the alternative) and $\sigma$s(for both), I conduct a log-likelihood ratio test. Likelihood values are calculated for 100 different data sets, each containing 200 data points, employing the specified convolved PDF. The calculation of each likelihood value necessarily involves integration, making the processing time-consuming. In analysing the aggregate data for the likelihood computations, I search for the parameter(s) that minimizes the negative likelihood.

*Minimisation: Minuit vs. Raster scan*

The minimisation process, which utilised the *iminuit* package, was unsuccessful in locating the correct minimum of the negative ln-likelihood. Despite attempts with varying limits and step sizes, there appeared to be a missing configuration within the *migrad* function that I was not accounting for. I am quite keen to find what causes *iminuit* not to find the right minimum. Consequently, I changed my approach to employ raster scanning as the method of minimisation. The resulting mean, median, and standard deviation for the estimated parameters obtained from the raster scans for both the null and alternative hypotheses are summarized in TableVI.
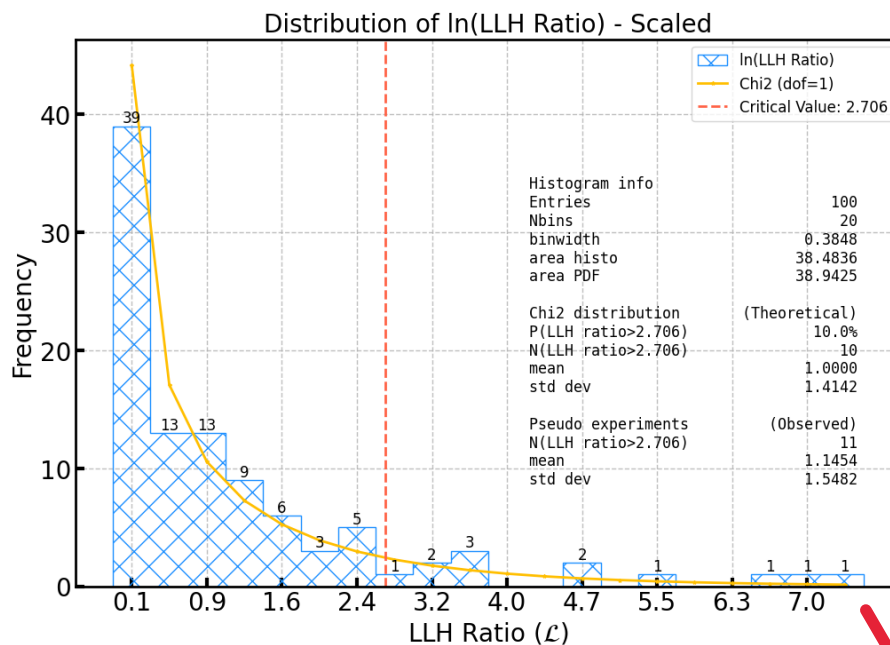
### The distribution of ln(likelihood ratio)

Now, I possess a set of 200 likelihood values for both the null hypothesis and the alternative hypothesis. From these sets, I compute 200 likelihood ratios, take the natural logarithm of each, and then multiply by -2. The resultant values are depicted in Figures22 and23. Given that the null hypothesis includes $\sigma$ and the alternative hypothesis comprises both $\sigma$ and $b$, and considering that the two $\sigma$ values originate from the same parameters of the underlying Gaussian distribution and show high correlation as indicated by the statistics in TableVI, it is reasonable to insist that the degrees of freedom (DOF) for this analysis is one. The distribution of ln(likelihood ratio) seems to conform to a chi-squared distribution with DOF=1. By comparing the statistical properties of the ratio's distribution with that of the chi-squared distribution, they manifest similar traits. This comparison is illustrated in the blank spaces of Figures22 and 23.

*Consistency above 2.706: Yes*

Given the distribution of the ratio follows the $\chi^2$ distribution with DOF = 1, I can calculate percentile position with respect to a specific value since the value has to do with the standard deviation of the normal distribution. For this instance, the proportion above 2.706 in the ratio or $\chi^2$ distribution is the same as the proportion of the area of the Gaussian curve with standard deviation $std = DOF$ outside the interval $[-\sqrt{2.706} \times (DOF), \sqrt{2.706} \times (DOF)]$, where $\sqrt{2.706} \sim 1.644$. The theoretical expectation value from the $\chi^2$ distribution (DOF=1) gives 10 while the ratio distribution result in giving 11. This discrepancy is rather minuscule considering the statistical characteristic of the two distributions that are shown in the blank space of Figure22 and 23.
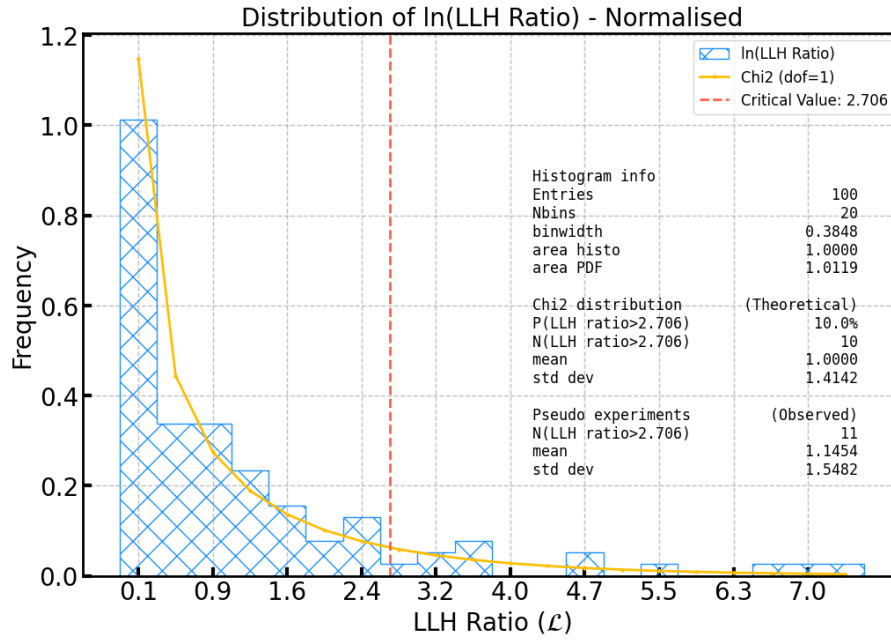
| Parameter | Mean | Median | Std Dev |
|---|---|---|---|
| $\sigma_0$ (Null) | 0.6136 | 0.6263 | 0.0555 |
| $\sigma_A$ (Alternative) | 0.6123 | 0.6263 | 0.0576 |
| $b_A$ (Alternative) | 0.9953 | 0.9737 | 0.0901 |

**Table VI:** Statistical measures for the parameters of null and alternative hypotheses.



**Figure 22:** The histogram of the natural log of the likelihood ratio. The $\chi^2$ distribution of degree of freedom = 1 is plotted on top.

**Figure 23:** Normalised distribution of ln(Likelihood Ratio), reflecting the frequency of the ratio values and their comparison to a $\chi^2$ distribution with one degree of freedom (dof=1). The dashed red line indicates the critical threshold for the likelihood ratio, aiding in the visual determination of significance levels.